

Conference Paper

Scattering Properties of a Suspension Containing Plate-like Particles and Their Aggregates

S. N. Chirikov¹ and A. V. Shkirin^{1,2}¹National Research Nuclear University MEPhI, Kashirskoe sh. 31, Moscow, 115409, Russia²Prokhorov General Physics Institute, Russian Academy of Sciences, ul. Vavilova 38, Moscow, 119991 Russia

Abstract

The results of the scattering matrix measurements at a wavelength of 0.63 μm are presented for an aqueous suspension of lead oxide containing plate-like particles and their aggregates with monomers dimensions of ~ 5 nm. The results of the measurements are compared with the matrix calculations for axially symmetric scatterers (ellipsoids of revolution). It is shown that the presence of aggregates affects the scattering properties of such a medium. The particles size distribution of the dispersed medium was found by solving the problem of minimizing the sum of the squares of the deviations of the experimental values of the matrix elements from calculated using the model of axially symmetric scatterers. It is demonstrated that the particle size distribution is more accurately retrieved by minimizing the sum of the squares of the deviations for the sum of the diagonal elements. The obtained distribution is compared with one measured by the dynamic light scattering method.

Corresponding Author:

S. N. Chirikov
snchirikov@mephi.ru

Received: 22 July 2018

Accepted: 9 September 2018

Published: 8 October 2018

Publishing services provided by
Knowledge E

© S. N. Chirikov and A. V. Shkirin. This article is distributed under the terms of the [Creative Commons Attribution License](#), which permits unrestricted use and redistribution provided that the original author and source are credited.

Selection and Peer-review under the responsibility of the Breakthrough Directions of Scientific Research at MEPhI Conference Committee.

Keywords: scattering matrix, aggregates, particle size distribution, axially symmetric scatterers, dynamic light scattering

1. Introduction

For laser methods for the diagnosis of disperse media based on detecting scattered radiation, high sensitivity and speed are characteristic; they are noninvasive and remote [1, 2]. Using these methods, the particle size distribution in a dispersed medium is found by solving the inverse scattering problem. For media containing spherical particles, these methods give reliable results, especially in the case of monomodal distribution of particles in a dispersed medium. Real media, as a rule, contain irregularly shaped particles of complex composition and structures, sometimes agglomerated and, in some cases, having a multimodal distribution. To consider the influence of these factors on the results of determining the parameters of disperse media the features

OPEN ACCESS

of scattering processes by complex media are being theoretically and experimentally investigated, and representative sets of model particle shapes is searched to simulate the scattering properties of such media. The registration of the polarization characteristics of the scattered radiation, namely, the elements of the scattering matrix (4×4), gives more complete information about the properties of disperse media in comparison with their determination from the scattering indicatrix or the correlation function [2]. In this article, the results of measurements of the scattering matrix of an aqueous suspension of lead oxide whose particles are plate-shaped are presented; and the possibility of reconstructing the distribution parameters of the particles of the dispersed phase by interpreting experimental data using the model of axially symmetric (spheroidal) scatterers is considered.

2. Methods and Equipment

An aqueous suspension of PbO particles was studied, the micrographs of which are shown in Figure 1. The refractive index of lead oxide is 2.61 [3], and PbO is considered to be a material that does not absorb radiation with a wavelength of $0.63 \mu\text{m}$. PbO particles are plates with rounded edges (Figure 1). Along with particles of coarse fraction (100–400 nm), the suspension contains fine particles (2–10 nm), which form aggregates. The histograms of the particle size distribution of the coarse and fine fractions are shown in Figure 2, where r is the radius of the circle having an area equal to the effective area of the particle. According to estimates (based on microphotographs), the fraction of coarse fraction is 10^{-4} – 10^{-5} .

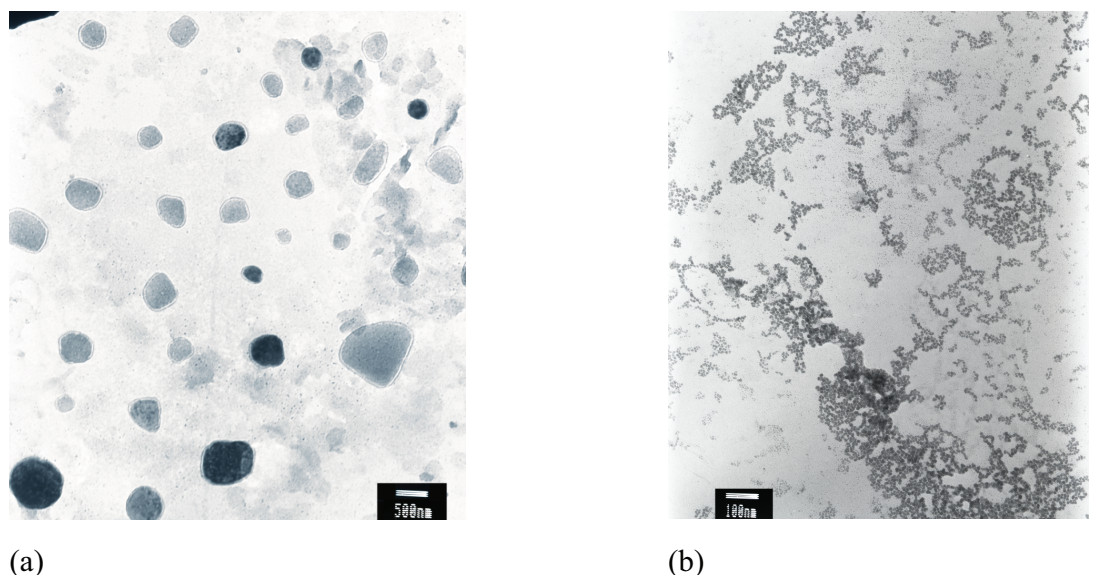


Figure 1: Microphotographs of particles of PbO, coarse fraction (a), aggregates (b).

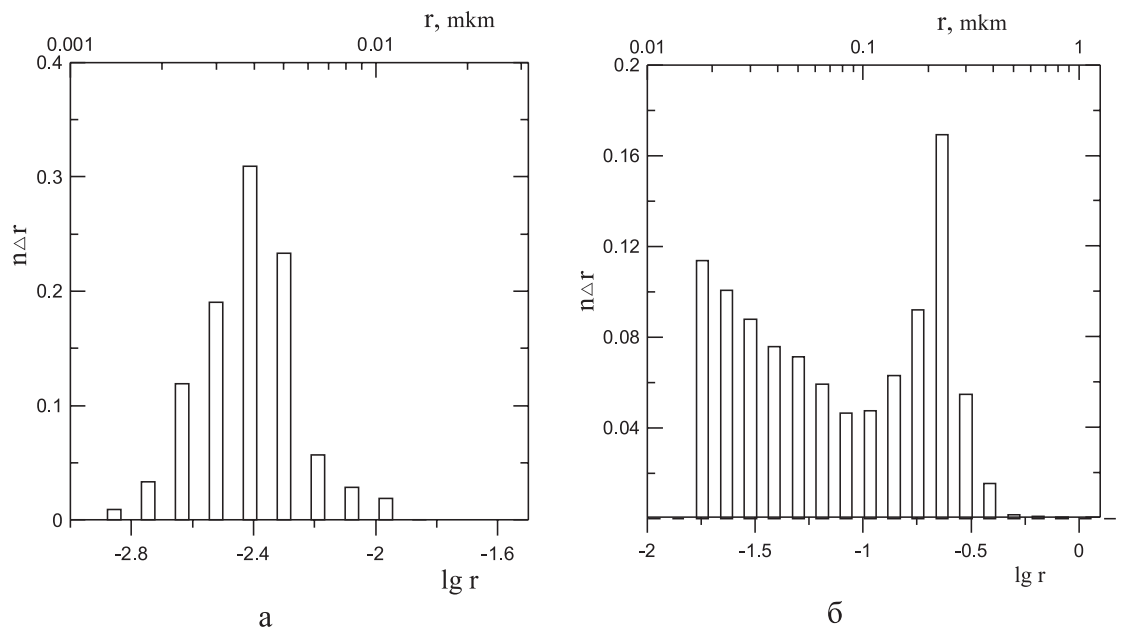


Figure 2: Histograms of particle size distribution of PbO, fine fraction (a), coarse fraction (b).

The scattering matrices were measured by laser polarimeter, where a single-mode He-Ne laser with a wavelength of $0.63 \mu\text{m}$ and a power of 7 mW was used as a radiation source. The measurements were carried out in the scattering angle range of 10° – 155° .

For a macroscopically isotropic medium that contains identical numbers of randomly oriented scatterers and their mirror-symmetric counterparts, scattering matrix $F(4 \times 4)$ has a block-diagonal form [2]. In this case, elements F_{14} , F_{41} , F_{24} , F_{42} , F_{31} , F_{32} , F_{13} , and F_{23} are zero and $F_{12} = F_{21}$, $F_{34} = -F_{43}$. The dependence of element F_{11} on angle of scattering θ describes the scattering indicatrix of the nonpolarized radiation. The measured scattering matrix was represented as a weighted sum of the theoretically calculated scattering matrices of model (spheroidal) particles with different sizes and shapes (aspect ratio b/c) and aggregated particles. The values of the corresponding weights that ensured a minimum of mean square deviations of the theoretical and experimental data determined the sought particle size distribution. The scattering matrices of spheroidal particles were calculated using the program that is based on the T-matrix method developed by Mishchenko M. I. [2] for an ensemble of randomly oriented spheroids.

When calculating the values of the elements F_{12} , F_{33} , F_{44} , F_{34} , the matrix elements of aggregates were assumed to be equal to the corresponding values of the elements of the Rayleigh matrix because of their small difference for aggregates with monomer sizes much smaller than the wavelength [4–6] and because the element F_{34} has approximately the zero value. Since, according to the data of [4], the values of the element

F_{22} for aggregates consisting of spheroidal monomers are close to the values of this element for spheroids of equivalent volume R_v , defined as the volume of a sphere with a radius:

$$R_v = \sqrt[3]{N} \cdot a \quad (1)$$

this they were used in calculations. In (1), N is the number of monomers in the aggregate, a is the radius of the sphere whose volume is equal to the volume of the monomer. The values of the element F_{11} and the scattering cross-section of aggregates were calculated in the Rayleigh-Debye-Gans approximation. The Levenberg-Marquardt algorithm was used to solve the optimization problem. The NanoTrac particle analyzer (Microtrac company), whose operating principle is based on the dynamic light scattering method (DLS), was also used to determine the particle size distribution. Particle sizes are determined by measuring the spectral density width of the backscattered electric field. Heterodyne detection scheme is employed; radiation reflected from the optode tip is used as a reference.

3. Results

The experimental dependences of the matrix elements on the scattering angle for the lead oxide suspension are shown in Figure 3. In it, f_{ij} are the matrix elements F_{ij} normalized on F_{11} ($f_{ij} = F_{ij}/F_{11}$). Using the model of axially symmetric scatterers, the experimental data were approximated, in which the matrix elements F_{ij} were represented as the sum of the contributions of particles of different types to the resulting scattering matrix:

$$F_{ij}^{teor}(\theta_k) = \frac{\sum_p \alpha_p \cdot C_p^{sca} \cdot F_{ij}^p(\theta_k)}{\sum_p \alpha_p \cdot C_p^{sca}}, \quad (2)$$

where θ_k is the scattering angle, α_p is the contribution of the corresponding type of particles to the scattering matrix, C_p^{sca} – the scattering cross-section, and F_{ij}^p are the matrix elements of the p -th kind of particles. In the approximation, the contributions α_i of particles of different sorts were determined, which ensures a minimum of the sum of the squared deviations of the theoretical values of all matrix elements from the experimental (Φ_1).

At the initial stage, the approximation problem was solved without considering the aggregation of particles. The scattering cross-sections of particles of coarse and fine fractions with sizes corresponding to the maxima of their distributions differ by nine

orders of magnitude, so one would expect that the main contribution to the dependences $f_{ij}(\theta)$ are determined by particles of coarse fractions. It should be noted that for particles whose dimensions are much smaller than the wavelength, the scattering matrix is Rayleigh, and its elements do not depend on the shape and size of the particles. The absence of a noticeable difference in the matrix elements for the first 15 ranges of histogram sizes in Figure 2 (because of the small particle size) does not allow during approximation considering all the ranges (Figure 2). Because of the practical equality of the elements of the first few columns of the Hessian matrix, it is impossible to calculate the inverse matrix. Therefore, the number of size ranges was reduced to 12 by eliminating the first 15 ranges from consideration. In the approximation, the number of particle kinds (p) was 48, which corresponds to the consideration of four different values of ε for 12 size ranges.

For the 16 sets of four ε values considered, the smallest values of the sum of the squares of the deviations were obtained during simulating the particles of the medium by oblate spheroids with a set of values $\varepsilon = 3,5,7,9$. The calculated dependences of the matrix elements on the scattering angle corresponding to this case are shown in Figure 3 (dashed lines). The differences between the calculated values of $f_{ij}(\theta)$ and the experimental values can be explained by the presence of aggregates of small particles of suspended matter.

To account for the presence of aggregates, the number of particle sorts considered in solving of the approximation problem was increased to 56, by adding aggregates. It was assumed that each aggregate consists of identical monomers – oblate spheroids with $\varepsilon = 5$ and size (radius of a sphere of equivalent volume) $a = 3$ nm, and their morphology can be described by the expressions:

$$N = k_0 \cdot \left(\frac{R_g}{a} \right)^{D_f} \quad R_g^2 = \frac{1}{N} \cdot \sum_{i=1}^N x_i^2, \quad (3)$$

where D_f is the fractal dimension, k_0 is the prefactor, R_g is the radius of the gyration, x_i is the distance from the i -th particle of the aggregate to its center of mass. It was assumed that the suspension contains aggregates that differ in the number of monomers and in the radius of the gyration. The prefactor value was considered equal to 1.2, and the fractal dimension varied in the interval 1.8–2.5.

For each representative set of particles, there were found contributions α_p , providing a minimum Φ_{1p} , and the value of this minimum. A representative set of particles consisted of spheroids with $\varepsilon = 3,5,7,9$ and aggregates having equal fractal dimension but possessing different sizes R_v in the range of 10–100 nm. For the six considered sets of particles that differ in the fractal dimension of the aggregates, the smallest value

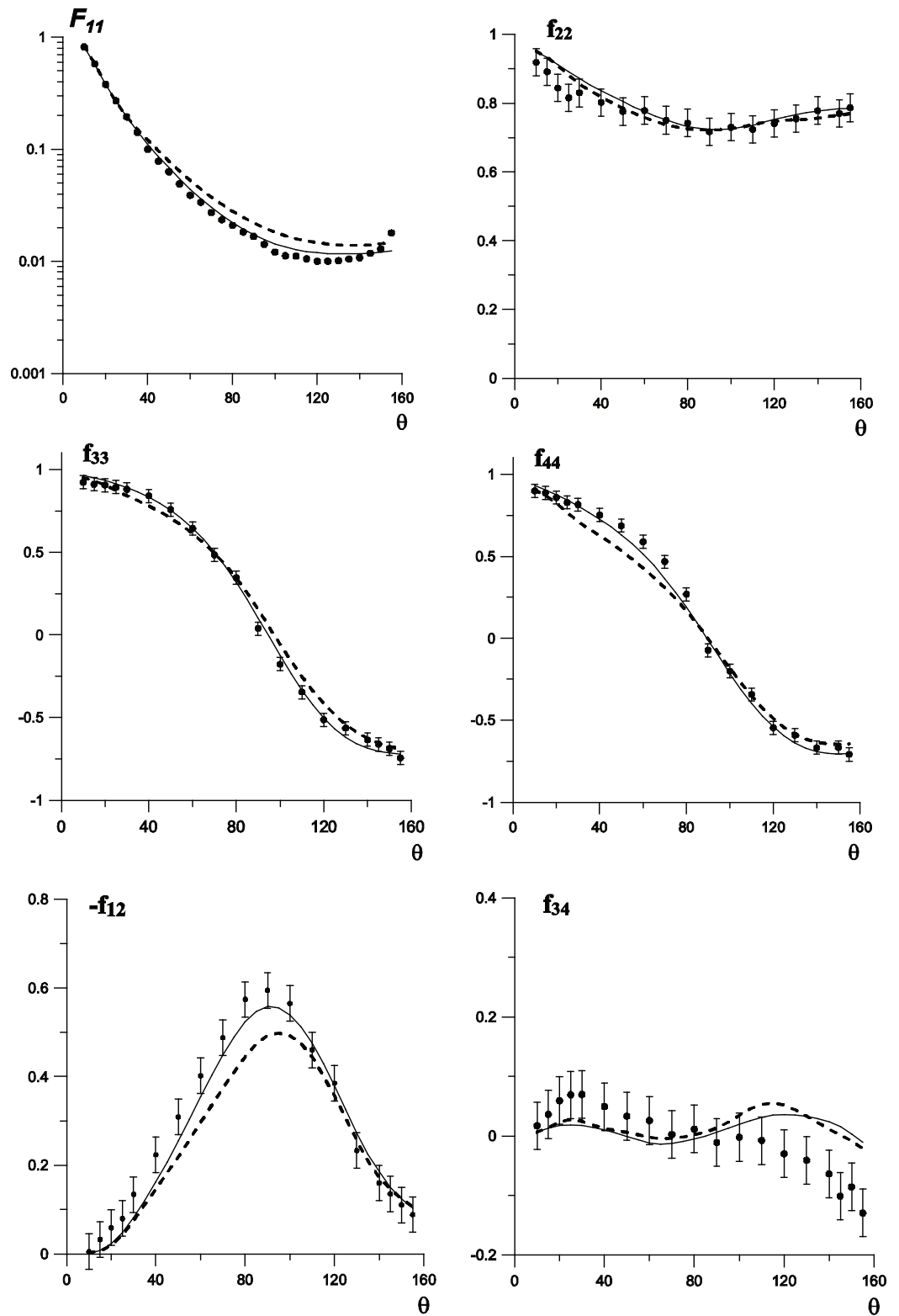


Figure 3: Dependences of matrix elements on the scattering angle for the PbO suspension. Dots are experimental data; lines are calculations without (dashed lines) and with (solid thin lines) considering the aggregation of particles.

of Φ_1 was obtained for a kit containing aggregates with $D_f = 2.3$. The corresponding

calculated dependences of the matrix elements on the scattering angle are shown in Figure 3 (solid lines). It is evident that considering the presence of aggregates when solving the approximation problem leads to a better agreement between the experimental and calculated data.

4. Discussion

Values of the contributions of particles of different kinds α_i , providing the smallest value of Φ_1 are shown in Figure 4 in the logarithmic (a) and linear (b) scale. Since according to the data of [7], the particle size distribution is more accurately reconstructed by minimizing the sum of the squared deviations of the diagonal elements of the matrix (Φ_2), then the same figure shows the contribution values for this case. On the vertical axis in Figure 4 shows the relative fraction of particles of a representative set with dimensions lying in the interval $r_i - r_i + \Delta r_i$. For aggregates, this is their relative share, and for spheroids, the sum of the contributions (α_p) of particles with different values of ϵ for each size range. For aggregates, the values of R_v are taken as their size. The size distribution obtained by minimizing the function Φ_2 more accurately reflects the actual, since it has a maximum in the region of the smallest particle sizes. For the retrieved distribution, the fraction of coarse fraction is 10^{-4} – 10^{-5} . It should be noted that in the distributions obtained, there is an extremum in the range of 200–400 nm corresponding to the maximum in the distribution of coarse fraction particles (Figure 2b), and an extremum in the range of 30–60 nm corresponding to the maximum in the distribution of aggregates.

The measurements made by the DLS method indicate the presence of a similar maximum in the distribution in the range of 30–50 nm (Figures 4c and 4d). The absence of a maximum in Figures 4c and 4d in the region of the smallest particle sizes (at $r < 20$ nm) is apparently due to the poor resolution of the DLS method and the fact that in the region of sizes 1–50 nm the dependence of the scattering cross-section on the particle size is very sharp. The absence of a maximum for particles of coarse fraction ($r = 100$ – 400 nm) in measurements by the DLS method is explained by the fact that the mathematical algorithm used in NanoTrack provides a determination of the share of particles $\geq 10^{-4}$. The discrepancy between the maxima of the distributions shown in Figures 4a, 4b, 4c, and 4d, in the range of 30–60 nm is due to the following circumstances. First, the particle model of the medium used to determine the particle size by the laser polarimetry method is approximate. This can include the shape deviation of the particles from the spheroidal, the presence of fine particle size distribution within

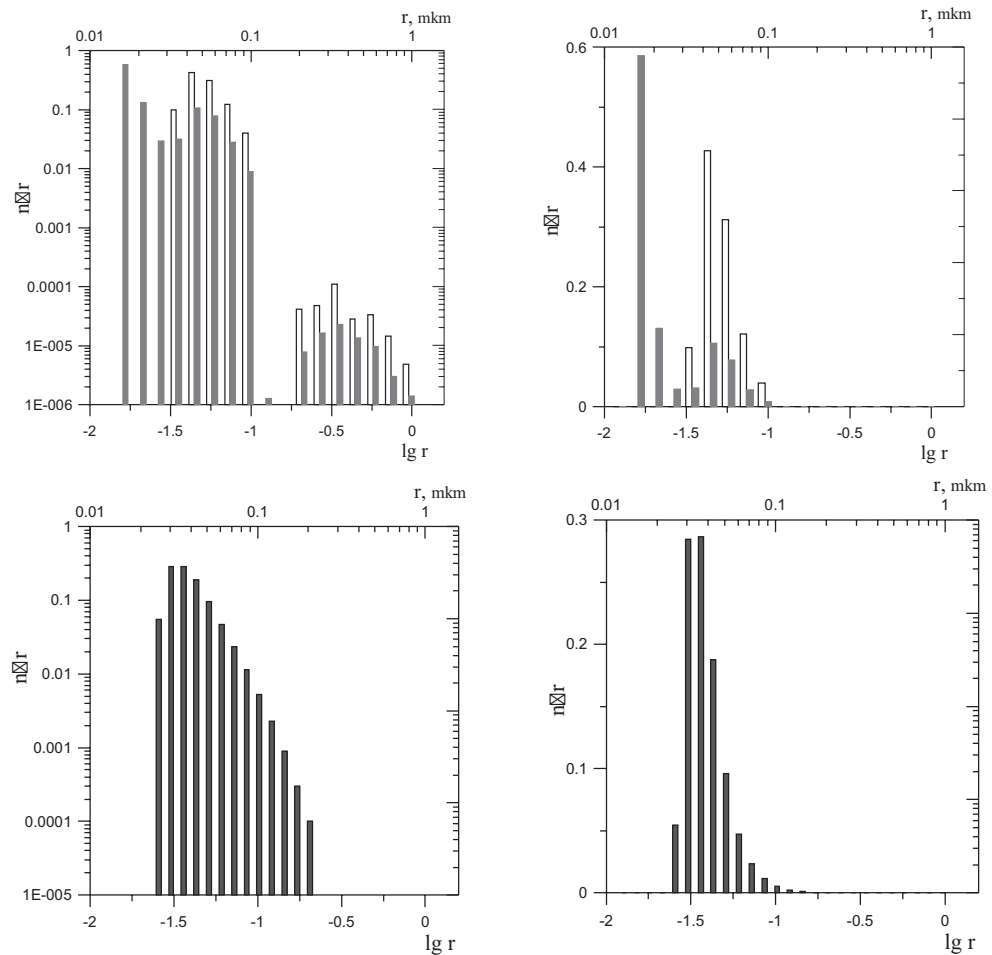


Figure 4: Histograms of particle size distribution in PbO defined by laser polarimetry (a, b) and DLS methods (c, d) in linear (b, d) and logarithmic (a, c) scales.

a single aggregate, the possible difference in the fractal dimensions of small and large aggregates. Secondly, using the DLS method, the distribution of the decay rates of the time correlation function is restored. The decay rate is determined by the diffusion of particles. Using model concepts of the dispersed medium and the relation of the diffusion coefficient with the particle size, one obtains their size distribution, assuming that the particles have a spherical shape. In this case, in determining the size of irregularly shaped particles, rotational diffusion and the influence on the diffusion coefficient of other processes (the interaction of the particles with one another, micromotions of the particles within a single macromolecule or the aggregate) are neglected. For media containing nonspherical particles or aggregates of particles, the measured distributions are approximate and require a correction that considers the specific features of the particular disperse medium.

5. Conclusion

For a dispersed medium containing plate-like particles and their aggregates of monomers with dimensions much smaller than the radiation wavelength, despite the large difference (nine orders of magnitude) of scattering cross-sections of coarse fraction particles and monomers forming aggregates, the presence of aggregates affects its scattering properties.

The use of a model of axially symmetric scatterers allows one to simulate with good accuracy the scattering properties of such a disperse medium.

Minimizing the sum of the squares of the deviations of the diagonal matrix elements measured and calculated in the framework of the spheroidal scatterers model allows us to retrieve the size distributions as for aggregates at the values of the parameter $2\pi R_v/\lambda > 0.1$, and for coarse fraction particles.

Acknowledgements

This work was supported by Competitiveness Growth Program of the Federal Autonomous Educational Institution of Higher Professional Education National Research Nuclear University MEPHI (Moscow Engineering Physics Institute).

References

- [1] Xu, R. (2002). *Particle Characterization: Light Scattering Methods*. New York: Kluwer Academic Publishers.
- [2] Mishchenko, M. I., Travis, L. D., and Lacis, A. A. (2002). *Scattering, Absorption, and Emission of Light by Small Particles*. Cambridge: Cambridge University Press.
- [3] Weber, M. J. (2003). *Handbook of Optical Materials*. New York: CRC Press LLC.
- [4] Wu, Y., Cheng, T., Zheng, L., et al. (2016). Effect of morphology on the optical properties of soot aggregated with spheroidal monomers. *Journal of Quantitative Spectroscopy and Radiative Transfer*, vol. 168, pp. 158–169.
- [5] Wu, Y., Gu, X., Cheng, T., et al. (2012). The single scattering properties of the aerosol particles as aggregated spheres. *Journal of Quantitative Spectroscopy and Radiative Transfer*, vol. 113, pp. 1454–1466.
- [6] Vilaplana, R., Luna, R., and Guirado D. (2011). The shape influence on the overall single scattering properties of a sample in random orientation. *Journal of Quantitative Spectroscopy and Radiative Transfer*, vol. 112, pp. 1838–1847.



- [7] Tymper, S. I. and Chirikov, S. N. (2015). Retrieval of particle size and shape distributions of TiO₂ and BaTiO₃ aqueous suspensions using measurement data on the scattering matrix. *Optics and Spectroscopy*, vol. 118, pp. 460–465.